Journal of Power Sources 227 (2013) 275–283

Contents lists available at SciVerse ScienceDirect

Journal of Power Sources

journal homepage: www.elsevier.com/locate/jpowsour

Cell performance modeling of direct methanol fuel cells using proton-exchange solid electrolytes: Effective reactant diffusion coefficients in porous diffusion layers

Bo-Yan Wang, Hun-Kai Lin [1], Nai-Yuan Liu, K.P.O. Mahesh, Shingjiang Jessie Lue*

Department of Chemical and Materials Engineering, Chang Gung University, Kwei-shan, Taoyuan 333, Taiwan

HIGHLIGHTS

- The developed mathematical model can predict direct methanol fuel cell performance.
- The model is validated using data at various operating conditions.
- This model can be extended to methanol fuel cells with various membranes.
- The model supplies a cost- and time-saving advantages for researchers.

ARTICLE INFO

Article history:
Received 30 May 2012
Received in revised form
1 November 2012
Accepted 12 November 2012
Available online 20 November 2012

Keywords:
Cell performance
Direct methanol fuel cell
Effective diffusion coefficients
Porous electrodes
One-dimensional mathematical model

ABSTRACT

The objective of this study is to develop a one-dimensional mathematical model for direct methanol fuel cell (DMFC) performance prediction. The modified model can be applied to DMFCs operated at wider ranges of methanol concentrations and temperatures with various solid electrolytes. Based on the model of Li et al. [J. Power Sources 154 (2006) 115–123], we propose a procedure to predict the effective diffusion coefficients of reactants (methanol and oxygen) in the diffusion layers to further estimate the limiting current densities. This approach does not use empirical fitting parameters and adopts the Darken equation and Boltzmann relationship to express the diffusivity dependency on the anode and cathode feed compositions. The diffusion layer porosity effect on the methanol and oxygen diffusion coefficients is accounted for using the Das equation. The proposed model is validated by experimental results obtained for 1–5 M of methanol feed at operating temperatures of 30–90 °C using Nafion, sulfonated poly(phthalazinone ether ketone), and sulfonated poly(ether ether ketone) electrolytes. The predictions are in good agreement with the experimental data. This model is helpful for researchers in estimating cell performance by eliminating the costs involved with preparing single cells during new material development.

1. Introduction

Direct methanol fuel cells (DMFCs) are a promising alternative power source, especially for portable electronic equipment, such as laptop computers, two-way radios, and mobile phones. DMFCs have the advantages of high energy density, low emission of pollutants, and the ability to use liquid fuel, which is easier to store and transport than hydrogen [1–4]. Moreover, fuel cells can be used as an emergency power supply because of their rapid start-up at ambient temperatures.

In the past decades, substantial research has been devoted to establishing models to better understand the phenomena arising within DMFCs. Most models consider the mass transport and electrochemical properties in a DMFC. Sundmacher and Scott reported on a one-dimensional model for DMFCs using a vaporized methanol feed [5]. Scott et al. [6–8] also developed a one-dimensional model for liquid-feed DMFCs that accounts for the methanol crossover and mass-transfer limitation at the catalyst surface. The influence of methanol crossover from the anode to cathode is based on a combination of diffusion, electroosmotic drag, and pressure. Kulikovsky [9,10] described a one-dimensional semi-empirical model for DMFC cell performance based on Tafel kinetics of the electrochemical reaction of methanol oxidation, the diffusion transport of methanol through the backing layer, and the

* Corresponding author. Tel.: +886 3 2118800x5489; fax: +886 3 2118700.
E-mail address: jessie@mail.cgu.edu.tw (S.J. Lue).
[1] Equal contribution to first author.

0378-7753/$ – see front matter © 2012 Elsevier B.V. All rights reserved.
http://dx.doi.org/10.1016/j.jpowsour.2012.11.029

methanol crossover. These models have several (5–9) fitting parameters and were solved under a narrow range of methanol feed concentrations (0–0.75 M). Eccarius et al. [11] used a design of experiments coupled with a mathematical model for a DMFC to study the influence of temperature, membrane thickness, methanol molarity, anode flow rate on methanol crossover, and leakage current density. Ko et al. [12] studied the numerical simulation results of a DMFC model and compared them with experimental results on the methanol crossover density of different Nafion membranes. Jeng and Chen [13] further defined the methanol concentration profile by introducing the void fractions of the diffusion and catalyst layers and the void fractions of Pt–Ru/C and ionomers in the catalyst layer. Kareemulla and Jayanti [14] used the multi-step reaction mechanism to describe the electrochemical oxidation of methanol at the anode and the Stefan–Maxwell equations for multi-component diffusion on the cathode side. Sun et al. [15] and Ge and Liu [16] introduced a three-dimensional, two-phase transport model for liquid-feed DMFCs. A review of the literature on DMFC models is presented by Oliveira et al. [17].

All the above models predict DMFC cell performance at low methanol concentrations, and most of the studies compare the modeling results with fuel cells using Nafion electrolyte. Some of the transport parameters are limited in the literature.

In this paper, we focused on developing a mathematical model to expand the applicability of DMFC performance prediction. The proposed model is based on the Kulikovsky model [9], which was later detailed by Li et al. [18]; however, our model incorporates analytical mass transfer parameters to precisely estimate the effective diffusion coefficients of methanol and oxygen in the diffusion layers. A benefit of this approach is that the reactant diffusion coefficient at certain feed compositions and cell temperatures can be used to predict the diffusivity under other operating conditions. This model takes into consideration various methanol concentrations, temperatures, and different solid electrolytes. Furthermore, the DMFC performance obtained by our model is validated using experimental data.

2. Model development

Our proposed mathematical model is based on the models proposed by Kulikovsky [9] and Li et al. [18] but uses mass-transfer characteristics from analytical equations. First, we adopted the Wilke–Chang estimation method [19], the Lennard-Jones potential model [20], and the equation of state of vapor–liquid equilibrium [21] to estimate the methanol and oxygen diffusion coefficients in the fluids. These diffusion coefficients were modified in accordance with the formula obtained by Das et al. [22] to calculate the effective diffusion coefficients of methanol and oxygen in the porous diffusion electrodes. The diffusion coefficients were used to predict the limiting current densities under various operating conditions. Finally, we applied the Kulikovsky [9] model to predict the cell voltages and to calculate the power densities in a DMFC using a 1–5 M methanol feed, operating temperatures ranging from 30 °C to 90 °C, and Nafion and other sulfonated solid electrolytes. The developed model is described in the following sections.

2.1. Conventional model

The overall reaction of a DMFC is:

$$CH_3OH_{(l)} + \frac{3}{2}O_{2(g)} \rightarrow CO_{2(g)} + 2H_2O_{(l)} \quad (1)$$

The assumptions for this model are described in the following sections:

(i) The cell is under isothermal conditions.
(ii) The methanol concentration in the anode catalyst layer is constant.
(iii) The electrode kinetics can be described using the Tafel equation.
(iv) Methanol crossover is mainly caused by diffusion in the membrane electrolyte; the electro-osmosis effect on the methanol transport rate through the membrane is negligible.
(v) The methanol concentration gradient is linear with respect to the trans-membrane direction inside the membrane.
(vi) The gas hold-up volume due to carbon dioxide evolution is negligible; the produced gas is immediately removed by the anode feed flow.
(vii) Membrane electrolyte resistance governs the ohmic voltage drop in the cell.
(viii) The oxygen pressure in the cathode catalyst layer is constant.
(ix) The reactions at the anode and cathode are first order.
(x) The concentration distributions are one-dimensional and only vary with respect to the trans-membrane direction.

The overpotential of a DMFC derived from Kulikovsky [9] and Li et al. [18] is expressed by the following equation:

$$V = E - \eta_a - \eta_\Omega - \eta_c \quad (2)$$

where E is the thermodynamic potential of a DMFC at a given operating condition, η_a is the overpotential at the anode described in Section 2.1.1, η_c is the overpotential at the cathode described in Section 2.1.2, and η_Ω is the ohmic potential drop in the cell. η_Ω is calculated as [9]:

$$\eta_\Omega = \frac{iL}{\sigma} \quad (3)$$

where i is the current density, L is the membrane electrolyte thickness, and σ is the ionic conductivity of the electrolyte. According to the Nernst equation, the thermodynamic cell potential at any given condition (E) is:

$$E = E^o - \frac{RT}{nF} \ln \frac{a_{CO_2} a_{H_2O}^2}{a_{CH_3OH} a_{O_2}^{\frac{3}{2}}} \quad (4)$$

where a is the activity of each reactant or product, R is the gas constant, T is the absolute temperature in Kelvin, n is the number of electrons in the half-reaction in a DMFC (6 in Eq. (1)), F is Faraday's constant, and E^o is the thermodynamic cell potential of the DMFC under standard conditions (a pure substance at 25 °C and 1 bar):

$$E^o = -\frac{\Delta G^o}{nF} \quad (5)$$

where ΔG^o is the Gibbs free energy change of the methanol oxidation reaction in Eq. (1). The predicted power density (P) of a DMFC was calculated as the product of the predetermined current density and the estimated cell voltage (from Eq. (2)):

$$P = iV \quad (6)$$

2.1.1. Anode overpotential

The anode overpotential (η_a) can be calculated by the combination of the kinetic reaction, mass transport, and methanol crossover as described in Eq. (7) [18,23]:

$$\eta_a = b_a \ln\left(\frac{i}{i_{ea}}\right) - b_a \ln\left(1 - \frac{i}{i_{la}}\right) + b_a \ln(1+\mu) \quad (7)$$

where b_a is the Tafel slope at the anode, i is the experimental current density, i_{ea} is the exchange current density at the anode, and i_{la} is the limiting current density of the anode and is defined as [24]:

$$i_{la} = 6F\frac{D_{ba}C_m}{L_{ba}} \quad (8)$$

where D_{ba} is the effective diffusion coefficient of methanol aqueous solution, L_{ba} is the thickness of anode diffusion layer, and C_m is the methanol feed concentration.

In Eq. (7), μ is a dimensionless parameter and is calculated as:

$$\mu = \frac{\beta}{L}\frac{L_{ba}}{D_{ba}} \quad (9)$$

where β is the methanol permeability of the membrane electrolyte. Wang and Wang demonstrated that the b_a and i_{ea} values are functions of temperature [24]:

$$b_a = \frac{RT}{0.8F} \quad (10)$$

and

$$i_{ea} = 94.25\left[\exp\left(\frac{35,570}{8.314}\right)\left(\frac{1}{273+80} - \frac{1}{T}\right)\right], \quad (11)$$

where 35,570 (in J mol^{-1}) is the activation energy derived by linear regression from the data of the performance of a DMFC that was composed of a 3.0 mg cm^{-2} Pt–Ru anode, a 3.4 mg cm^{-2} Pt cathode, and a Nafion-117 electrolyte. The value of 8.314 (in J mol^{-1} K^{-1}) represents the gas constant. These relationships were established at 60–100 °C using 1 M methanol (4 mL min^{-1}) and 2.07 × 10^5 Pa (30 psig) air at 1800 sccm [25].

2.1.2. Cathode overpotential

The cathode overpotential (η_c) caused by the diffusional mass-transfer limitation due to a loss in oxygen concentration can be estimated from the combination of the kinetic reaction, mass transport, and methanol crossover using the following equation:

$$\eta_c = b_c \ln\left(\frac{i}{i_{ec}}\right) - b_c \ln\left(1 - \frac{i}{i_{lc}} - R_c\right) \quad (12)$$

where b_c is the Tafel slope at the cathode, i_{ec} is the exchange current density of the cathode, i_{lc} is the limiting current density at the cathode, and R_c is a dimensionless parameter accounting for the potential drop due to the methanol crossover [24]. The i_{lc} and R_c values were obtained using the following equations:

$$i_{lc} = 4F\frac{D_{bc}C_O}{L_{bc}} \quad (13)$$

where D_{bc} is the diffusion coefficient of oxygen in the cathode backing layer, L_{bc} is the thickness of the cathode backing layer and C_O is the oxygen feed concentration, and

$$R_c = \frac{i_{la}}{i_{lc}}\left(\frac{\mu}{1+\mu}\right)\left(1 - \frac{i}{i_{la}}\right) \quad (14)$$

The b_c and i_{ec} values depend on the cell temperature [24]:

$$b_c = \frac{RT}{0.7F} \quad (15)$$

and

$$i_{ec} = 0.04222\left[\exp\left(\frac{73,200}{8.314}\right)\left(\frac{1}{273+80} - \frac{1}{T}\right)\right] \quad (16)$$

This relationship is based on an activation energy of 73,200 J mol^{-1} for a DMFC, conducted between 30 and 80 °C [26] using Nafion-117 sandwiched between Pt microelectrodes. The membrane characteristics play important roles in the cell performance. For instance, electrolyte conductivity (σ), methanol permeability (β), and membrane thickness (L) are shown in Eqs. (3) and (9). The data are further entered to Eqs. (2), (12) and (14) to demonstrate their impacts on the fuel cell voltage.

2.2. Modified model

The equations stated in Section 2.1 were adopted in the modified model for DMFC performance prediction with parameter adjustments. The solid electrolyte conductivity (σ) as a function of temperature (T) is described as follows:

$$\sigma = \sigma_{ref} \exp\left[1268\left(\frac{1}{T_{ref}} - \frac{1}{T}\right)\right] \quad (17)$$

where σ_{ref} is the conductivity at a reference temperature (T_{ref}) [27]. The D_{ba} and D_{bc} values were adjusted using the procedure described in the following sections.

2.2.1. Methanol diffusion coefficient at the anode

The methanol diffusion coefficient in aqueous solution was estimated using the Darken equation [28,29]:

$$D_{MW} = \left(D^o_{MW}x_M + D^o_{MW}x_W\right)\alpha, \quad (18)$$

where D_{MW} is the methanol diffusion coefficient in water from methanol solutions, D^o_{ij} is the diffusion coefficient of solute I in an infinite dilute solution of solvent J, and M and W denote methanol and water, respectively. The x_M and x_W values are the methanol and water molar fractions, respectively. The parameter α is a thermodynamic correction term given by the following equation [30]:

$$\alpha = \left(\frac{\partial \ln a_M}{\partial \ln x_M}\right)_{T,P} \quad (19)$$

where a_M and x_M are the activity and mole fraction of methanol, respectively. The D^o_{WM} and D^o_{MW} values were predicted using the Wilke–Chang equation for the diffusion coefficients of solutes in solvents at infinite dilution [19]:

$$D^o_{WM} = \frac{7.4\times10^{-8}(\Phi_M M_M)^{1/2}T}{\zeta_M v_W^{0.6}} \quad (20)$$

and

$$D^o_{MW} = \frac{7.4\times10^{-8}(\Phi_W M_W)^{1/2}T}{\zeta_W v_M^{0.6}} \quad (21)$$

where M is the solvent molecular weight, v is the solute molar volume at its boiling temperature, ζ is the solvent viscosity, T is the temperature, and Φ is the association factor of the solvent (2.6 for water and 1.9 for methanol [19]).

The correction term α in Eq. (19) was acquired from the vapor–liquid equilibrium data of methanol and water [21] using UNIQUAC parameters. The ln a_M and ln x_M from 30 to 80 °C are plotted in Fig. 1. From the slope, we obtained α values of 0.9704, 0.9419, 0.9146, and 0.8639 for 1 M, 2 M, 3 M, and 5 M methanol solutions, respectively, at 30 °C. As the temperature increased, the α values slightly decreased. For instance, the α values were 0.9594, 0.9211, 0.8851, and 0.8206 for 1 M, 2 M, 3 M, and 5 M methanol solutions, respectively, at 80 °C.

By substituting appropriate methanol concentrations and temperatures, we obtained corresponding methanol diffusion coefficients in water. Then, the effective methanol diffusion coefficient in the porous diffusion layer was calculated as [22,31]:

$$D_{MW}^{eff} = \left(1 - \left(\frac{3(1-\theta_a)}{3-\theta_a}\right)\right) D_{MW} \tag{22}$$

where θ_a is the porosity of the anode diffusion layer. The experimental methanol diffusion coefficient at 90 °C has been reported to be 1.8×10^{-5} cm^2 s^{-1} with a b_a of 0.3 mm [9]. This value was used to calculate the apparent porosity θ_a (which was estimated to be 0.406). The predicted effective methanol diffusion coefficient was used as D_{ba} in Eqs. (8) and (9) to estimate the anode overpotential described in Section 2.1.1.

2.2.2. Oxygen diffusion coefficient into cathode

The oxygen diffusion coefficient in air at the cathode was estimated using the simplified Boltzmann equation [30]:

$$D_{OA} = \frac{0.00266T^{1.5}}{pM_{OA}^{0.5}\sigma_{OA}^2\Omega_D} \tag{23}$$

where T is the temperature, p is the oxygen pressure, M_{OA} is the equivalent molar mass (defined in Eq. (25)), Ω_D is the dimensionless diffusion collision integral presented in Eq. (26)), and σ_{OA} is the characteristic Lennard-Jones length (Å) and is taken as the average of oxygen and air data:

$$\sigma_{OA} = \left(\frac{\sigma_O + \sigma_A}{2}\right) \tag{24}$$

where σ_O and σ_A data were obtained from the literature [28]. M_{OA} is the equivalent molar mass, defined as [30]:

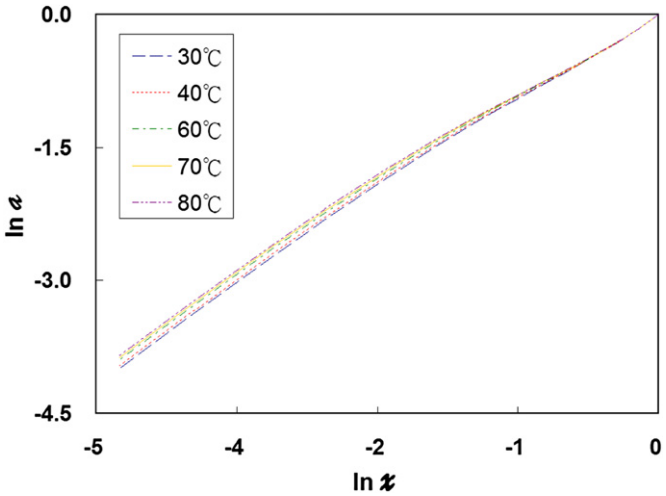

Fig. 1. Plots of ln a_M compared with ln x_M for methanol solutions at 30–80 °C. The slopes at any methanol mole fraction correspond to the α value defined in Eq. (15).

$$M_{OA} = 2\left[\left(\frac{1}{M_O}\right) + \left(\frac{1}{M_A}\right)\right]^{-1} \tag{25}$$

where M_O and M_A are the molar masses of oxygen and air, respectively. Ω_D is the diffusion collision integral [32]:

$$\Omega_D = \frac{1.06036}{(T^*)^{0.1561}} + \frac{0.193}{\exp(0.47635T^*)} + \frac{1.03587}{\exp(1.52996T^*)} + \frac{1.76474}{\exp(3.89411T^*)} \tag{26}$$

where T^* (reduced temperature) equals $\kappa T/\varepsilon_{OA}$, κ is Boltzmann's constant, and ε_{OA} is the characteristic Lennard-Jones energy presented in the following equation:

$$\varepsilon_{OA} = (\varepsilon_O \varepsilon_A)^{1/2} \tag{27}$$

where ε_O and ε_A are the characteristic Lennard-Jones energies of oxygen and air [30].

The effective oxygen diffusion coefficient (D_{OA}^{eff}) in the porous gas diffusion layer was calculated as [22]:

$$D_{OA}^{eff} = \left(1 - \left(\frac{3(1-\theta_c)}{3-\theta_c}\right)\right) D_{OA} \tag{28}$$

where θ_c is the porosity of the cathode gas diffusion layer. The experimental effective diffusion coefficient of oxidant at the cathode at 90 °C has been reported to be 0.9×10^{-3} cm^2 s^{-1} [10] when L_{bc} is 0.3 mm. This value was used to calculate the apparent porosity θ_c. Once the apparent porosity is known, the effective gas diffusion coefficient in the porous electrode can be determined and used to estimate the cathode overpotential (described in Section 2.1.2).

3. Experimental

3.1. Electrolyte preparation

The Nafion-117 membrane (from DuPont Co., Fayetteville, North Carolina, USA) was first boiled with hydrogen peroxide (5 wt%, Riedel-de Haen, Seelze, Germany) for 1 h to remove organic matters. It was rinsed in pure water for 0.5 h. Then, the Nafion was boiled in H_2SO_4 (1 M, Riedel-de Haen, Seelze, Germany) for 1 h to ensure complete conversion to an H-type exchange membrane and rinsed again with pure water. The pure water was produced using a Millipore water purifier (RiOs-5 and Millipore-Q Gradient, Millipore Corp., Bedford, Massachusetts, USA).

The sulfonated poly(phthalazinone ether ketone) (SPPEK) powder with an ion-exchange capacity of 1.42 meq g^{-1} was obtained from FuMA-Tech GmbH (Fumion® P-700, Ingbert, Germany). In total, 1 g of SPPEK was dissolved in 9 g of dimethylformamide (DMF) with continuous stirring for one day. The solution was filtered through Advantec filter paper (No. 1, Advantec MFS, Inc., Dublin, CA, USA) to obtain a clear solution. The polymer solution was cast on a glass plate and the solvent was allowed to evaporate in a ventilation hood for 3 days. The film was then dried at 80 °C in a vacuum oven for 24 h. The dry film was peeled off and immersed in 1 M H_2SO_4 (Riedel-de Haen, Seelze, Germany) for 1 h to ensure complete conversion to H-type exchange membrane and was rinsed again with pure water.

3.2. Conductivity and methanol permeability measurements

The tested membrane electrolyte was immersed in deionized water or methanol solutions for 3 h at various temperatures and

held between two stainless steel electrode rods in a glass T-tube, as described in our previous paper [33]. The specimen was maintained at 95% relative humidity at a predetermined temperature for the conductivity measurement. An alternate-current impedance spectrum was obtained using a potentiostat (Autolab PGSTAT 30ZN potentiostat, Eco Chemie B.V., Utrecht, The Netherlands). The impedance was scanned at 10^6 Hz–10^{-1} Hz at an applied voltage of 10 mV. Nyquist plots were used to extract the conductivity values of the electrolytes, as described in our previous report [33].

The methanol permeability was determined using a hand-made, double-jacked, glass permeation cell. The glass cell was divided into two compartments. One reservoir was filled with a 1 M methanol aqueous solution, and the other receiving reservoir was filled with deionized water. The membrane was placed between these two compartments and the methanol transport through the membrane was measured by the concentration increase in the receiving reservoir with time. The methanol concentration was measured using a gas chromatograph (HP 4890A, Agilent Technologies Co. Ltd., St. Louis, MO, USA). The experimental set-up and calculation of the methanol permeability were described in our previous publication [34].

3.3. Fuel cell test

The membrane electrolyte was sandwiched between the sheets of the gas diffusion electrodes (E-tek, 6 mg cm^{-2} Pt–Ru for the anode and 5 mg cm^{-2} Pt for the cathode) to obtain a membrane electrode assembly (MEA). The active area of the MEA electrode was 5 cm^2. Two heating tapes were adhered to the surfaces of the end plates. The thermostated methanol solution was fed into the anode at a flow rate of 2 mL min^{-1}, and humidified oxygen gas was fed into the cathode at a flow rate of 80 mL min^{-1}. A thermocouple was inserted into the end plates, and the measured temperature was fed back to a controller to ensure that the cell temperature was at the set point. The electrochemical measurements of the DMFCs were recorded using the constant current density mode with an electrical load (PLZ164 WA electrochemical system, Kikusui Electronics Corporation, Tokyo, Japan). The experimental set-up of the fuel cell test was reported previously [35].

4. Results and discussion

4.1. Effect of diffusion layer porosity on cell performance

The diffusion layer porosity has a profound impact on the effective reactant diffusion coefficients in the diffusion layers (Eqs. (22) and (28)) and on the cell voltage (Eq. (2)). Fig. 2 plots the predicted cell voltage as a function of the current density with the same porosity value for the anode and cathode diffusion layers using the modified DMFC model, which was fed with 1 M methanol and 1-bar pure oxygen at 60 °C. When the porosities were both 0.1 for the anode and cathode diffusion layers, the predicted voltage values were the lowest among the tested parameters.

As the diffusion layer porosities increased beyond 0.4, the cell voltages increased, in particular for current densities beyond 70 mA cm^{-2} (Fig. 2). Moreover, the polarization curves with porosities of 0.4–0.9 were almost undifferentiated, which implies that the predicted cell voltage was nearly independent of porosity for values higher than 0.4. The predicted polarization curves were in accordance with the experimental data (Fig. 2), except for the low current density (<50 mA cm^{-2}) range. In the literature [6,7,12,13,16,24,36,37], porosity values of 0.3–0.875 were adopted in establishing models for predicting DMFC performance; the selection of this parameter value only plays a minor role based on our results presented in Fig. 2.

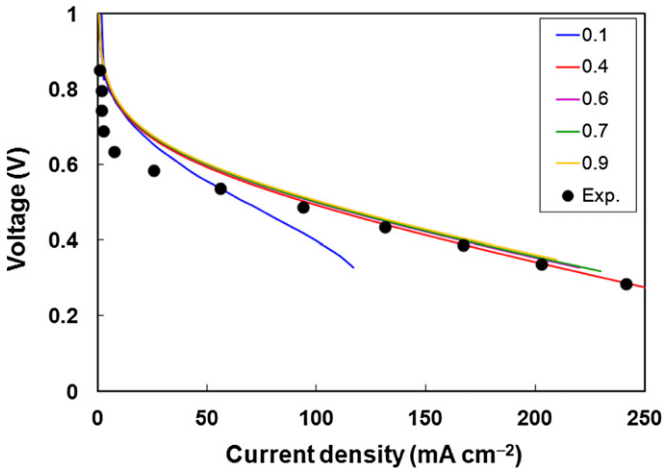

Fig. 2. Predicted voltage–current density curves using the modified model with the same porosities (0.1–0.9) for anode and cathode in a DMFC fed with 1 M methanol and pure oxygen at 60 °C. The experimental data (Exp.) are shown for comparison.

Next, we set the anode and cathode porosities to different values to examine their individual impacts on cell performance. The modeling was performed for a DMFC fed with 1 M methanol and pure 1-bar oxygen at 60 °C. When the cathode porosity was set at 0.12 and the anode porosity varied from 0.1 to 0.9, the predicted cell voltage was higher with a higher anode porosity (Fig. 3(a)). The estimated peak power density (P_{max}) increased from 41.7 to 74.5 mW cm^{-2} as the anode porosity increased from 0.1 to 0.9. When the cathode porosity was set at 0.41 and the anode porosity varied from 0.1 to 0.9, the predicted cell voltage also increased with a higher anode porosity (Fig. 3(b)). These polarization curves were similar to those in Fig. 3(a) at the same anode porosity value, and the estimated P_{max} was less than 0.5% deviation from the results using a cathode porosity of 0.12. This finding indicates that the cathode porosity is not a governing factor in cell performance.

With the anode porosity set at 0.41 and 0.12, the predicted polarization curves are illustrated in Fig. 4(a) and (b), respectively. At an anode porosity of 0.41, the generated current density reached at least 300 mA cm^{-2} (Fig. 4(a)) with an estimated P_{max} of 70 mW cm^{-2}, regardless of the cathode porosity values. As the anode porosity decreased to 0.12, the predicted polarization curves demonstrated a severe mass-transport potential loss beyond a current density of 100 mA cm^{-2} (Fig. 4(b)). The predicted P_{max} was 42 mW cm^{-2}, a 40% reduction from the value obtained for an anode porosity of 0.41. Again, the data confirm that the anode porosity is more influential than the cathode porosity.

4.2. Comparison between the proposed and conventional Kulikovsky model

Fig. 5 presents the DMFC polarization curves using the conventional Kulikovsky model [38] and our modified model, along with experimental data for comparison. Fig. 5(a) consists of the experimental data and the model predictions using a Nafion-117 membrane electrolyte and fed with 1 M methanol as the anode feed at 70 °C. The modified model fits well with the experimental data reported by Ge and Liu [39], whereas the Kulikovsky model suggests much lower cell voltage and power density values. The P_{max} values obtained using the Kulikovsky model and our modified model were 76 and 83.4 mW cm^{-2}, respectively. The latter was closer to the experimental value of 86.7 mW cm^{-2}. The percentage errors for using the Kulikovsky model and the modified model

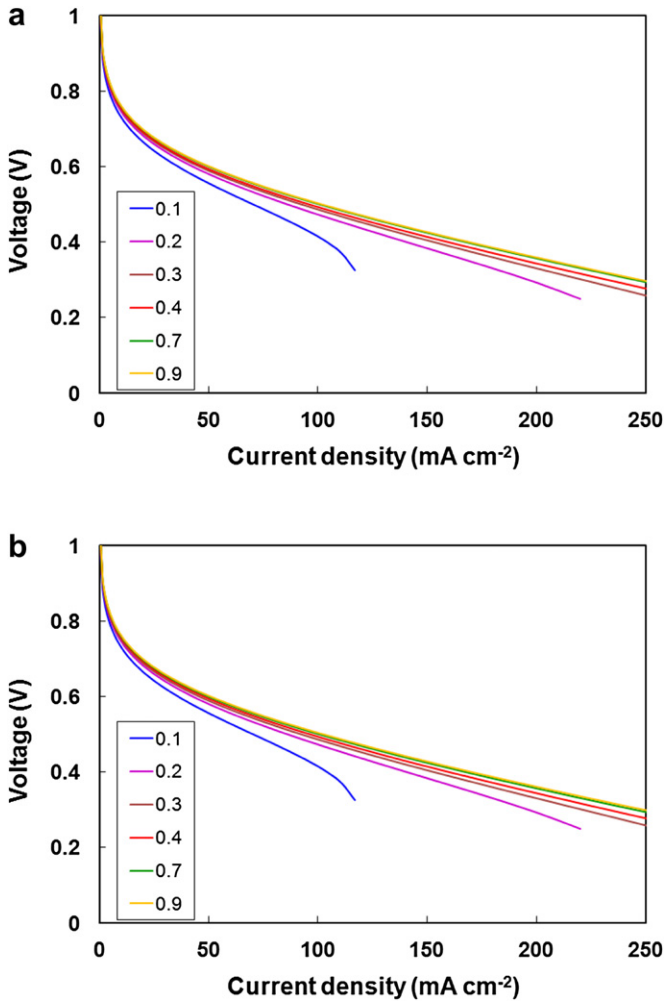

Fig. 3. Predicted polarization curves using the modified model for DMFCs with a porosity of (a) 0.12 and (b) 0.41 for the cathode diffusion layer and various porosities for the anode diffusion layer. (The cell was fed with 1 M methanol and pure oxygen at 60 °C and was equipped with a Nafion-117 electrolyte.)

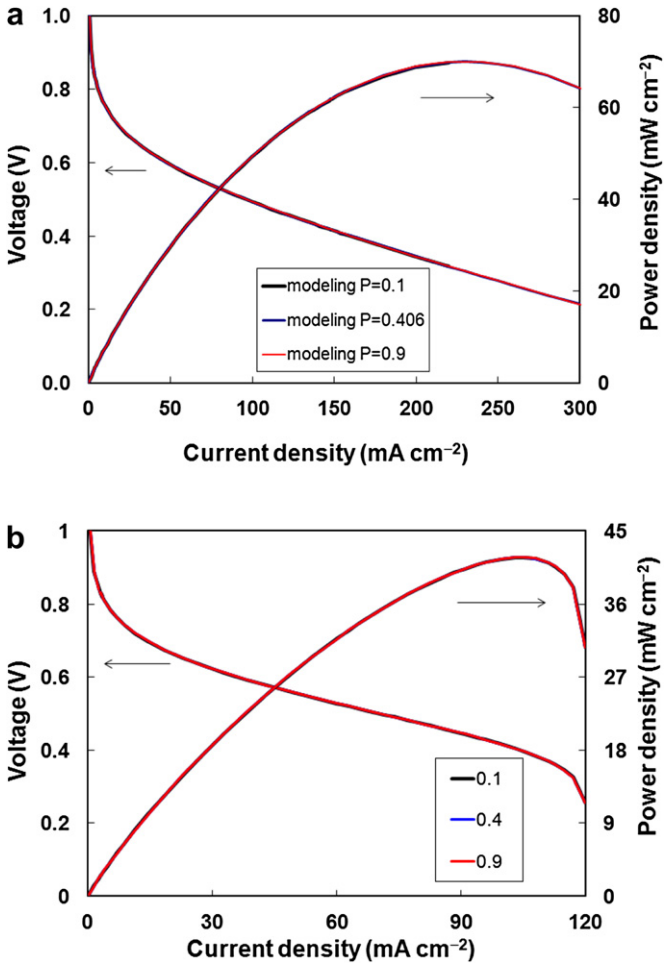

Fig. 4. Predicted polarization curves using the modified model for DMFC with a porosity of (a) 0.41 or (b) 0.12 at the anode diffusion layer and various porosities at the cathode diffusion layer. (The cell was fed with 1 M methanol and pure oxygen at 60 °C and was equipped with Nafion-117 electrolyte.)

were 12.3 and 3.8%, respectively. Except for the low current density regions, the modified model agrees well with the experimental data. Our modified model provides precise estimates of cell voltage and power density for DMFCs.

4.3. Effect of temperature on cell performance using the modified model

The proposed mathematical model for DMFC performance was also compared with the experimental data at 80 °C and 90 °C using a Nafion membrane and a 1 M methanol anode feed. The experimental results were obtained from Gurau and Smotkin [40], Scott et al. [41], Wu and Zhang [42], and Witham et al. [43] and are plotted in Fig. 5(b) and (c). The voltage and power density cure pattern of the modified model for the Nafion membrane were in agreement with the experimental values of Gurau and Smotkin [40] and Scott et al. [41]. Again, the modified model outperformed the conventional model.

Fig. 6(a) and (b) plots the predicted cell voltage and power density as functions of current density using the modified model for DMFCs equipped with Nafion at 40–90 °C to verify the accuracy of the modified model. As the cell temperature increased from 40 °C to 90 °C, P_{max} increased from 48.8 to 112.14 mW cm^{-2}. This increase resulted from the higher Nafion conductivity associated with a higher temperature, leading to a slower decline in ohmic loss (Fig. 6(a)). The predicted P_{max} data using the modified model were in excellent agreement with the experimental results for the entire temperature range, as demonstrated in Fig. 6(c). One of the main contributions of this approach is to predict DMFC performance for different temperatures as long as the diffusion layer porosity data are available. Other determinations are based on theoretical mass-transfer equations. One feasible approach is to estimate the porosity from one temperature at which the effective diffusion coefficients are determined. By assuming that the porosities are not significantly affected by the temperature change, the porosity values can be used to estimate the effective diffusivity at other temperatures using the procedure outlined in Section 2.2.

4.4. Effect of methanol concentration on cell performance using modified model

Fig. 7(a) and (b) plots the polarization curves and the power densities obtained using the modified model for DMFCs with Nafion membrane with different methanol feed concentrations at 70 °C. The measured methanol permeability from various concentrations was 7.77×10^{-6}, 8.15×10^{-6}, 8.52×10^{-6}, and 1.25×10^{-5} cm^2 s^{-1} for 1, 2, 3, and 5 M, respectively, at 70 °C. The estimated P_{max} values for 1, 2, 3,

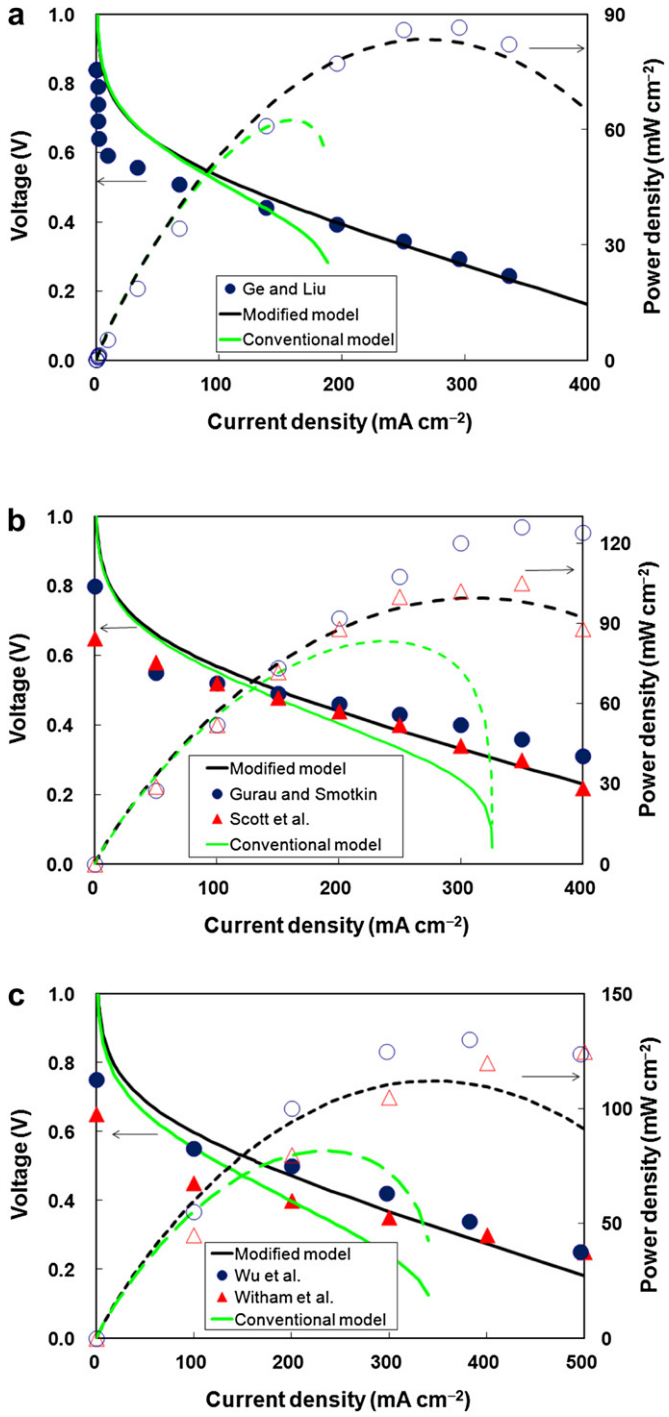

Fig. 5. Conventional and modified model predictions and comparison with experimental data at various temperatures. The cell was fed with 1 M methanol and pure oxygen and was equipped with a Nafion-117 electrolyte. (a) 70 °C, experimental data from Ref. [39]; (b) 80 °C, experimental data from Refs. [40,41]; (c) 90 °C, experimental data from Refs. [42,43].

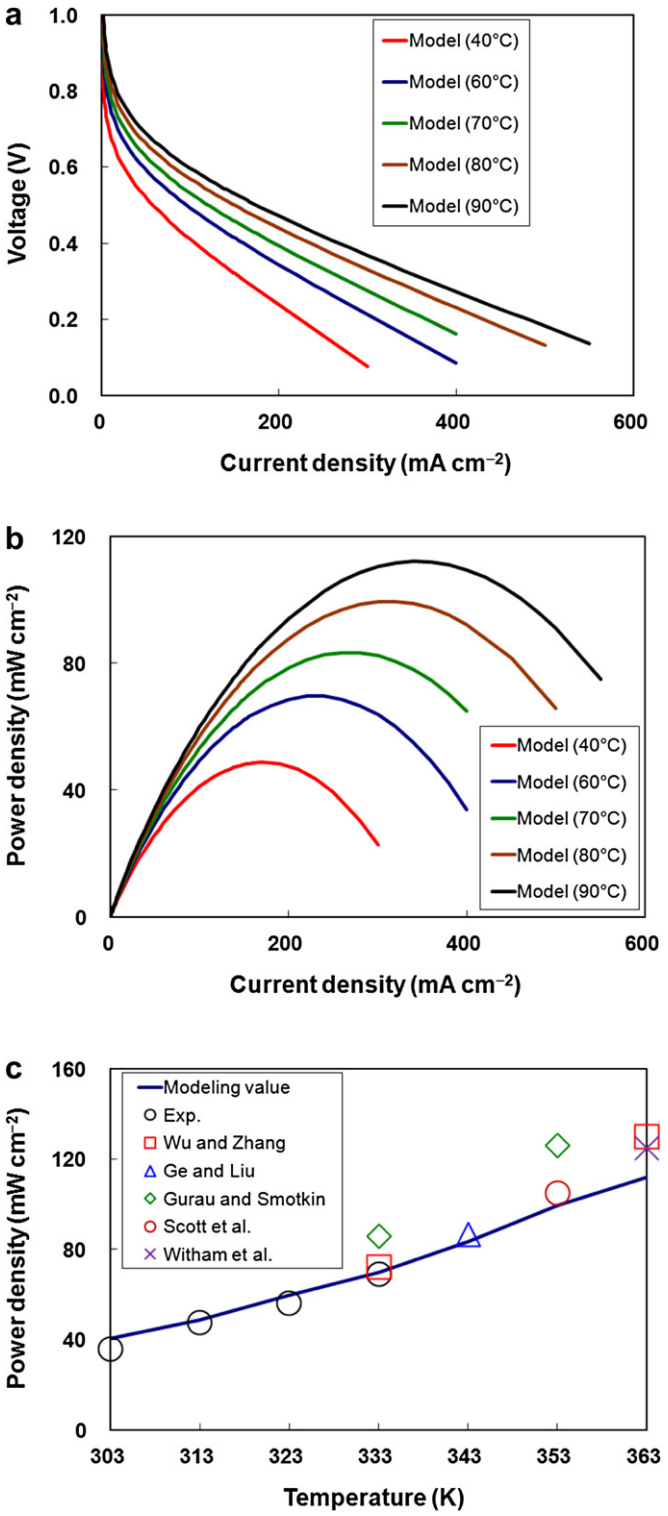

Fig. 6. Predicted (a) polarization curves, (b) power densities, and (c) peak power density data along with the experimental values (cited from Refs. [39–43] and our measurements) of DMFCs at 30–90 °C using the modified model. (The cell was fed with a 1 M methanol solution, pure oxygen, and Nafion-117).

and 5 M methanol feeds were 85, 99, 115, and 110 mW cm^{-2} at 70 °C. Compared with the experimental data reported by Ge and Liu [39] under comparable conditions, the P_{max} values were 87, 132, 137, and 128 mW cm^{-2}, respectively, at the corresponding methanol concentrations. The modified model predicted enhanced cell voltage and power density with increasing methanol concentration, although the concentration effect is more profound in the experimental data. On average, the modified model predictions deviated by approximately 16% from the data presented by Ge and Liu [39]. Further investigation is suggested to improve the model accuracy by incorporating parameters associated with the high methanol concentrations.

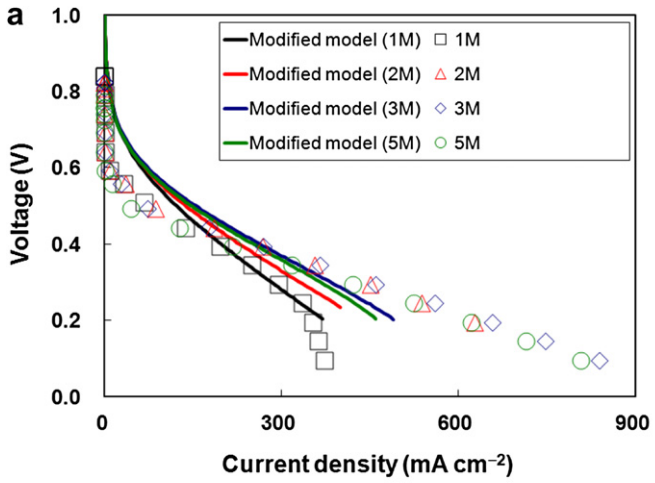

Fig. 7. Predicted (a) polarization curves and (b) power density results using the modified model for DMFCs at 70 °C and fed with a methanol aqueous solution of various concentrations [39].

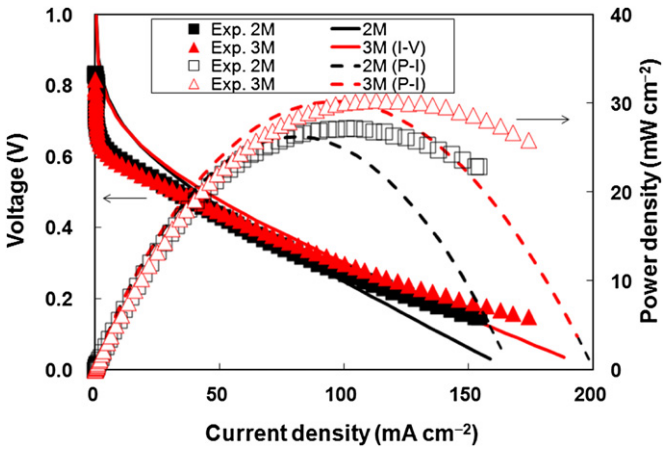

Fig. 8. Predicted polarization curves (left axis) and power density results (right axis) using SPPEK electrolyte in DMFC (fed with 2 M or 3 M methanol solution, oxygen at cathode, operated at 60 °C).

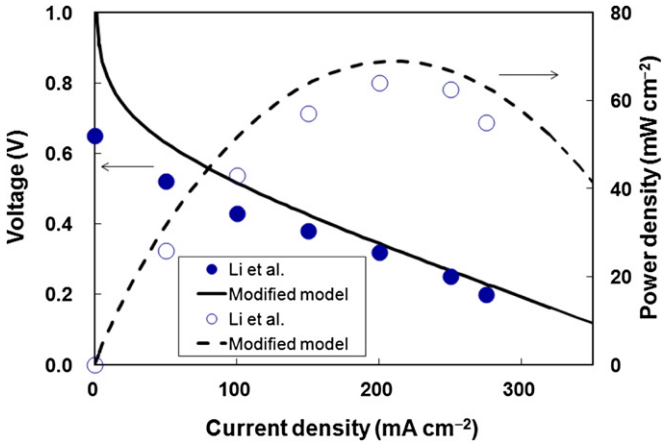

Fig. 9. Predicted polarization curves (left axis) and power density results (right axis) using SPEEK electrolyte in DMFC (fed with 2 M methanol solution, oxygen at cathode, operated at 80 °C). Electrolyte characters and cell performance data are from Li et al. [44].

4.5. Modeling for other membrane electrolytes

The DMFC experimental results using the sulfonated poly(-phthalazinone ether ketone) (SPPEK) were used to verify the versatility of the modified model. This electrolyte was prepared and characterized in house. Fig. 8 presents the DMFC performance predictions and the experimental data using the SPPEK with 2 M and 3 M methanol feeds at 60 °C. The estimated P_{max} using the SPPEK was 26.2 mW cm^{-2}, matching the experimental result of 27 mW cm^{-2} with the 2 M methanol feed. For the 3 M methanol feed, the P_{max} prediction was 30.2 mW cm^{-2}, in agreement with the experimental value of 30.4 mW cm^{-2}. The predicted peak power density results for both the 2 M and 3 M methanol feeds are almost identical to the experimental results. This agreement confirms the accuracy and versatility of the modified model.

We also validated our proposed model using data presented by Li et al. [44]. These researchers prepared and characterized a sulfonated poly(ether ether ketone) (SPEEK) membrane, followed by determining DMFC performance using this solid electrolyte. Fig. 9 illustrates the prediction and experimental results for the cell voltage and power density for the DMFC using the SPEEK electrolyte. The peak power density prediction was 69 mW cm^{-2}, slightly higher than the experimental value (64 mW cm^{-2}). However, the error was less than 7.3%. This example demonstrates that given the characteristics of the electrolyte (thickness, conductivity, and methanol permeability), one can apply our modified model to estimate the DMFC performance. This modeling process provides cost-saving advantages by eliminating unnecessary fuel cell preparation and testing experiments, particularly by reducing the usage of expensive catalysts and electrolytes. Preliminary data on fuel cell performance can be simulated with sufficient precision using this model.

5. Conclusion

The effective diffusion coefficients of reactants in the porous diffusion layers were estimated using the Wilke–Chang equation, the Lennard-Jones potential model, and the UNIQUAC equation for vapor–liquid equilibrium data on methanol/water solutions. The data were adopted into a conventional Kulikovsky model to estimate the polarization curve and power density of a DMFC. Therefore, the prediction has a theoretical basis without the requirement of any fitting parameters. The model was validated using experimental results obtained using a 1–5 M methanol feed, operating temperatures at 30–80 °C, with Nafion and other solid electrolytes.

This model was able to predict the effects of diffusion layer porosity, cell temperature, and methanol concentration on cell performance using various electrolyte membranes. The data in Figs. 2 and 5–9 illustrate the precision of the predictions (shown in lines) against experimental results from various sources (shown in symbols). The simulation model provides a valuable development tool with cost- and time-saving advantages for researchers.

References

[1] N. Nakagawa, Y. Xiu, J. Power Sources 118 (2003) 248–255.
[2] A.S. Aricò, S. Srinivasan, V. Antonucci, Fuel Cells 1 (2001) 133–161.
[3] C.Y. Chen, P. Yang, J. Power Sources 123 (2003) 37–42.
[4] C.K. Dyer, J. Power Sources 106 (2002) 31–34.
[5] K. Sundmacher, K. Scott, Chem. Eng. Sci. 54 (1999) 2927–2936.
[6] K. Scott, W. Taama, J. Cruickshank, J. Power Sources 65 (1997) 159–171.
[7] K. Scott, P. Argyropoulos, K. Sundmacher, J. Electroanal. Chem. 477 (1999) 97–110.
[8] G. Murgia, L. Pisani, A.K. Shukla, K. Scott, J. Electrochem. Soc. 150 (2003) A1231–A1245.
[9] A.A. Kulikovsky, Electrochem. Commun. 5 (2003) 1030–1036.
[10] A.A. Kulikovsky, Electrochem. Commun. 4 (2002) 939–946.
[11] S. Eccarius, B.L. Garcia, C. Hebling, J.W. Weidner, J. Power Sources 179 (2008) 723–733.
[12] J. Ko, G. Lee, Y. Choi, P. Chippar, K. Kang, H. Ju, J. Power Sources 196 (2011) 935–945.
[13] K.T. Jeng, C.W. Chen, J. Power Sources 112 (2002) 367–375.
[14] D. Kareemulla, S. Jayanti, J. Power Sources 188 (2009) 367–378.
[15] P. Sun, G. Xue, C. Wang, J. Xu, A combined finite element-upwind volume-Newton's method for liquid-feed direct methanol fuel simulations. 6th international fuel cell science, engineering and technology conference, June 16–18, 2008, Dever, Colorado, USA, 1–14.
[16] J. Ge, H. Liu, J. Power Sources 160 (2006) 413–421.
[17] V.B. Oliveira, D.S. Falcao, C.M. Rangel, A.M.F.R. Pinto, Int. J. Hydrogen Energy 32 (2007) 415–424.
[18] X. Li, E.P.L. Roberts, S.M. Holmes, J. Power Sources 154 (2006) 115–123.
[19] C.R. Wilke, P. Chang, AIChE J. 19 (1973) 264–270.
[20] J.O. Hirschfelder, C.F. Curtiss, R.B. Bird, Molecular Theory of Gases and Liquids, Wiley, New York, 1954.
[21] J.M. Smith, H.C. Van Ness, M.M. Abbott, Introduction to Chemical Engineering Thermodynamics, McGraw-Hill Book, Boston, 2005.
[22] P.K. Das, X. Li, Z.S. Liu, Appl. Energy 87 (2010) 2785–2796.
[23] J. Divisek, J. Fuhrmann, K. Gärtner, R. Jung, J. Electrochem. Soc. 150 (2003) A811–A825.
[24] Z.H. Wang, C.Y. Wang, J. Electrochem. Soc. 150 (2003) A508–A519.
[25] S. Gottesfeld, M.S. Wilson, in: T. Osaka, M. Datta (Eds.), Energy Storage Systems for Electronics, Gordon and Breach Science Publishers, Singapore, 2000, pp. 487–519.
[26] A. Parthasarathy, S. Srinivasan, A.J. Appleby, C.R. Martin, J. Electrochem. Soc. 139 (1992) 2530–2537.
[27] T.V. Nguyen, R.E. White, J. Electrochem. Soc. 140 (1993) 2178–2186.
[28] L.S. Darken, Trans. Am. Inst. Mining Metall. Eng. 175 (1948) 184–201.
[29] R.K. Khai, H. Ertel, F.A.L. Dullien, AIChE J. 19 (1973) 881–900.
[30] R.C. Reid, J.M. Prausnitz, B.E. Poling, The Properties of Gases and Liquids, McGraw-Hill Book, New York, 1988.
[31] N. Zamel, N.G.C. Astrath, X. Li, J. Shen, J. Zhou, F.B.G. Astrath, H. Wang, Z.S. Liu, Chem. Eng. Sci. 65 (2010) 931–937.
[32] P.D. Neufeld, A.R. Janzen, R.A. Aziz, J. Chem. Phys. 57 (1972) 1100–1102.
[33] S.J. Lue, W.T. Wang, K.P.O. Mahesh, C.C. Yang, J. Power Sources 195 (2010) 7991–7999.
[34] S.J. Lue, H.J. Juang, S.Y. Hou, Sep. Sci. Technol. 37 (2002) 463–480.
[35] S.J. Lue, K.P.O. Mahesh, W.T. Wang, J.Y. Chen, C.C. Yang, J. Membr. Sci. 367 (2011) 256–264.
[36] T.E. Springer, T.A. Zawodzinski, M.S. Wilson, S. Golfesfeld, J. Electrochem. Soc. 143 (1996) 587–599.
[37] P. Argyropoulos, K. Scott, W.M. Taama, Electrochim. Acta 44 (1999) 3575–3584.
[38] A.A. Kulikovsky, J. Electrochem. Soc. 153 (2006) A1672–A1677.
[39] J. Ge, H. Liu, J. Power Sources 142 (2005) 56–69.
[40] B. Gurau, E.S. Smotkin, J. Power Sources 112 (2002) 339–352.
[41] K. Scott, W.M. Taama, P. Argyropoulos, J. Appl. Electrochem. 28 (1998) 1389–1397.
[42] J.J. Wu, Y.J. Zhang, J. Shijiazhuang Univ. 7 (2005) 13–16.
[43] C.K. Witham, W. Chun, T.I. Valdez, S.R. Narayanan, Electrochem. Solid-state Lett. 3 (2000) 497–500.
[44] L. Li, J. Zhang, Y. Wang, J. Membr. Sci. 226 (2003) 159–167.

Nomenclature

a: activity of reactant or product (–)
b_a: Tafel slope at anode (V)
b_c: Tafel slope at cathode (V)
C_m: methanol concentration (mol cm^{-3})
C_O: oxygen concentration (mol cm^{-3})
D^o: solute diffusion coefficient at infinite dilution (cm^2 s^{-1})
D_{ba}: methanol diffusion coefficient in anode diffusion layer (cm^2 s^{-1})
D_{bc}: oxygen diffusion coefficient in cathode diffusion layer (cm^2 s^{-1})
D_{ij}: diffusion coefficient of component I in mixture with J (cm^2 s^{-1})
D^{eff}: effective diffusion coefficient of reactant in porous diffusion layer (cm^2 s^{-1})
E: thermodynamic cell potential at any condition (V)
E^o: thermodynamic cell potential at standard state (V)
F: Faraday's constant (96,485 C mol^{-1})
ΔG^o: Gibbs free energy change in overall reaction for a DMFC at standard state (J mol^{-1})
i: current density (A cm^{-2})
i_{ea}: exchange current density for anode (A cm^{-2})
i_{ec}: exchange current density for cathode (A cm^{-2})
i_{la}: limiting current density at the anode (A cm^{-2})
i_{lc}: limiting current density at the cathode (A cm^{-2})
L_{ba}: thickness of backing layer at the anode (cm)
L_{bc}: thickness of backing layer at the cathode (cm)
L: thickness of electrolyte (cm)
M: molar mass (g mol^{-1})
n: number of electrons in half-reaction
P: power density (mW cm^{-2})
p: gas pressure (bar)
R: gas constant (8.314 J mol^{-1} K^{-1})
R_c: dimensionless parameter accounting for potential drop due to methanol cross-over (–)
T: temperature (K)
T^*: reduced temperature (–)
V: cell voltage (V)
v: molar volume (cm^3)
x: mole fraction (–)

Greek
α: thermodynamic correction term (–)
β: methanol permeability (cm^2 s^{-1})
ε: characteristic Lennard-Jones energy (J)
ζ: solvent viscosity (cP)
η_a: overpotential at the anode (V)
η_c: overpotential at the cathode (V)
η_Ω: ohmic potential drop (V)
θ: porosity of diffusion layer (–)
κ: Boltzmann's constant (J K^{-1})
μ: dimensionless parameter (–)
σ: proton conductivity of solid electrolyte membrane (S m^{-1})
σ_{OA}: characteristic Lennard-Jones length (Å)
Φ: solvent association constant (–)
Ω_D: diffusion collision integral (–)

Subscript
a: anode
A: air
c: cathode
M: methanol
O: oxygen
ref: reference
W: water